

Conduction-electron g -factor measurements in platinum

P. Gustafsson, H. Ohlsén, and L. Nordborg

Department of Solid State Physics, Institute of Technology, Uppsala University, Box 534, S-751 21 Uppsala, Sweden

(Received 16 May 1985)

The de Haas—van Alphen effect has been used to study the Zeeman splitting of the Landau levels for the closed Γ sheet and the α orbit on the open hole sheet in platinum. From the spin-splitting zeros of both the fundamental and second harmonic together with the variation of the amplitude, the anisotropy of the Zeeman splitting has been mapped out in the symmetry planes. The change of integer between spin-splitting-zero contours has been established through studies of an iron-diluted platinum crystal. The area around [110] has been investigated in great detail for the Γ sheet, revealing a large anisotropy in the Zeeman splitting. In contrast to the anisotropy of the Γ sheet the g_c factor of the α orbit appears to be almost isotropic. The anisotropy of the cyclotron-orbit g_c factor is discussed in view of band-structure properties and compared with earlier presented results on palladium.

INTRODUCTION

The spin splitting of the Landau levels caused by a magnetic field has been studied in several types of elements for some years now. The orbital g_c factor, which is used to characterize the spin splitting, has been investigated with regard to a possible shift from the free-electron value of 2 and an anisotropy with respect to the crystallographic directions, which are thought to originate from the spin-orbit interaction and many-body effects.

The de Haas—van Alphen (dHvA) effect is very useful for such measurements since its amplitude depends on the g_c factor through a cosine function with argument $k\pi R$, where k is the harmonic number of the dHvA signal and R is the ratio between the Zeeman splitting energy and the Landau-level spacing¹ and can be expressed as $g_c m_c / 2$; m_c is the cyclotron effective mass expressed in units of the free-electron mass. The g_c factor is unique for each orbit on a specific sheet. This is different from the averaged bulk values which can be found through magnetic susceptibility and conduction-electron spin-resonance measurements.

Since g_c appears in a cosine function, there is an ambiguity in its absolute value. For metals where exchange enhancement is not expected to have any influence on the g_c factor, the value closest to 2 is commonly chosen and any deviation from 2 is interpreted as a consequence of spin-orbit or electron-electron interactions. For the transition elements the exchange enhancement is not negligible and will to some extent increase the g_c factor.² Even if the absolute value of g_c cannot be obtained, the dHvA effect offers a unique opportunity to measure its anisotropy.

Two techniques which exploit the dHvA effect have been used in this work for studying g_c . The spin-splitting-zero (SSZ) technique makes use of the vanishing of the amplitude, which occurs whenever $R = n + \frac{1}{2}$, n being an integer. With several SSZ contours over the Fermi surface, a good picture of the anisotropy of g_c can be gained, especially if any change of n between neighboring

contours can be resolved. In the absolute-amplitude technique the measured amplitudes are compared with the calculated Lifshitz-Kosevich (LK) values.³ The ratios will then give the values of $\cos(\pi R)$.

Our work is concerned with the spin splitting on the closed Γ sheet and for the α orbit on the open hole sheet in platinum. In an earlier paper⁴ the wealth of SSZ contours for the fundamental on the Γ sheet was revealed together with several SSZ's for the second harmonic of the dHvA signal. In this work one additional SSZ contour on the Γ sheet has been mapped out and a study of a platinum crystal diluted with a small amount of iron has given the changes of the integer n between the different contours.

As pointed out earlier, the g_c factor can be affected both by the spin-orbit interaction and by many-body effects. Unfortunately, there have been few theoretical works on this subject, and since the experimental studies have become more extended, the gap between experimental results and theoretical models remains. Furthermore, the theoretical contributions have dealt with point g factors in k space even though the orbital g_c factor is the meaningful concept when the band structure is perturbed by a magnetic field. It is not yet clear to what extent the anisotropy of g_c in exchange-enhanced metals comes from the spin-orbit interaction or from many-body effects. The results in a previous paper on palladium⁵ together with the results reported in this paper should constitute a basis for comparison with calculations of the influence on g_c from different effects.

EXPERIMENTAL TECHNIQUE AND ANALYSIS

The measurements were performed in a cryogenic system that allows observations in a magnetic field of 6.5 T and a temperature of 0.55 K. In this system the sample can be rotated 180° with a resolution of 0.1° around an axis perpendicular to the magnetic field. One additional degree of freedom is introduced as the magnet can be tilted $\pm 3.5^\circ$, making it possible to align symmetry directions

with the magnetic field to better than 0.2° . The field-modulation technique was used with a modulation frequency of 210 Hz and the eighth harmonic was used for detection of the Γ sheet and the fourth harmonic for the α orbit.

The pure platinum single crystal was grown in an electron-beam zone refiner. The starting material, a 99.999%-pure platinum 1-mm wire, was zone-refined 20 times before the single crystal was grown. A 1-mm-long sample was spark-cut from the single-crystal rod and etched in hot *aqua regia*. The diluted platinum crystal was made by melting a platinum wire together with a small amount of iron powder in a radio-frequency heater. This iron-diluted platinum wire was then homogenized in the electron-beam zone refiner by letting the zone pass up and down several times. A single crystal was grown and cut as above. Atomic absorption analysis of the parts of the wire next to the sample crystal gave an iron content of 100 ppm.

Two different numerical methods have been used for studying the second harmonic of the dHvA oscillations. The second harmonic consists of a pure LK part and a magnetic interaction (MI) part which can be extracted when the phase between the fundamental and the total second harmonic is found.⁶ The ratio between the MI part and the LK part is proportional to $F^2 T \coth(\beta m_c T/B)/B^{5/2}$, where F is the dHvA frequency, B the magnetic field, T the temperature, and $\beta = 14.69 \text{ TK}^{-1}$. This makes it favorable to study the second harmonic on small orbits. In platinum the α orbit is sufficiently small to make the second harmonic almost pure LK, even at such a relatively low field as 6.5 T. For the Γ sheet the squared frequency term makes the MI increase by a factor of 100 compared with the value for the α orbit. Despite this, the analysis of the second harmonic in parts of the investigated Γ sheet has given results that are consistent and reliable. However, in the region where the α orbit exists as a strong signal, it causes a frequency modulation of the Γ signal which prevents a thorough study of the second harmonic. One numerical method fitted the recorded amplitudes to a sum of sine and cosine functions by varying a trial dHvA frequency until the least-squares sum was minimized. Another method used was a standard Fourier transform to find the amplitudes and phase relations. For both methods 250–300 data samples were taken on eight to ten oscillations, giving equivalent results.

RESULTS

The most accurate determination of R is done in the directions of SSZ's. This method is often somewhat restricted since nature has not provided the elements with a great number of SSZ's, though studies of higher dHvA harmonics may make the method fruitful. In platinum several contours and parts of contours of SSZ's for both the fundamental and second harmonic of the dHvA oscillations have been mapped out (Fig. 1). Even if this method gives an estimate of the variation of R , it has to be completed. We have measured the amplitude between the SSZ contours, and from a comparison with a calculat-

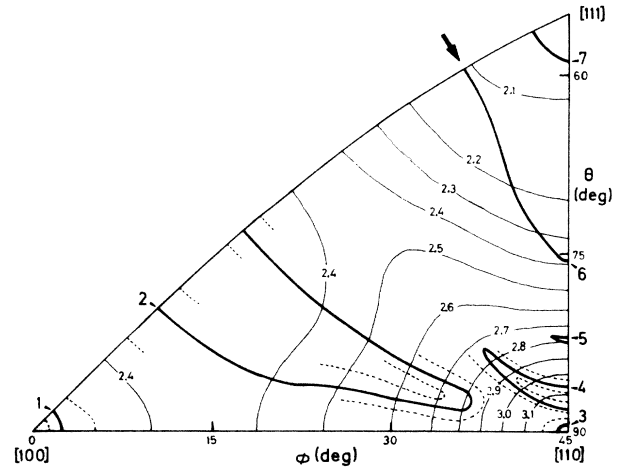


FIG. 1. Stereographic plot in the basic irreducible $\frac{1}{48}$ th wedge of the Brillouin zone of SSZ contours and branches of contours for the fundamental (thick solid lines) and second harmonic (dashed line) on the Γ sheet. The thin solid lines are contours of constant effective masses from Ref. 7. The newly observed SSZ contour for the off-center orbit is marked by an arrow and all contours for the fundamental are labeled by integers.

ed amplitude from the LK theory³ the values of the spin-splitting factor were extracted. For this comparison the SSZ's of the second harmonic were used for a calibration of the amplitude. At these positions $|\cos(\pi R)| = 1/\sqrt{2}$.

The Γ sheet

The (100) plane is crossed by two SSZ contours for the fundamental. We have found that the values of R for these contours differ by one with the higher value for the contour around [110]. Close to the contours of the fundamental there are three SSZ contours for the second harmonic, two at [100], and one around [110]. The SSZ contours are concentrated around the symmetry directions, while the main part of the plane is not connected with any detailed information of this type about the variation of R . Therefore the amplitude was measured in the mirror plane in steps of 0.5° under constant experimental conditions. This measured amplitude was then compared with the calculated LK amplitude, for which the area and effective-mass variation were taken from the work of Ketterson and Windmiller⁷ and the curvature factors were computed using the radii given in the same paper. The Dingle temperature was measured at [100] and considered constant with angle. From the values of the spin-splitting factors extracted in this way, the variation of R was evaluated. In Fig. 2 we present a graph of $R(\theta, \phi)$ to connect the R values at the symmetry directions.

The variation of $R(\theta, \phi)$ in the (110) plane has been mapped out most carefully from [100] out to 26° in Ref. 1. We have continued that work and the investigation can be divided into three parts.

(i) The first part is from the third SSZ of the fundamental from [100] out to 38° in the (110) plane, where the off-center orbit splits off and coexists with the central orbit in the area around [111]. One may notice that when

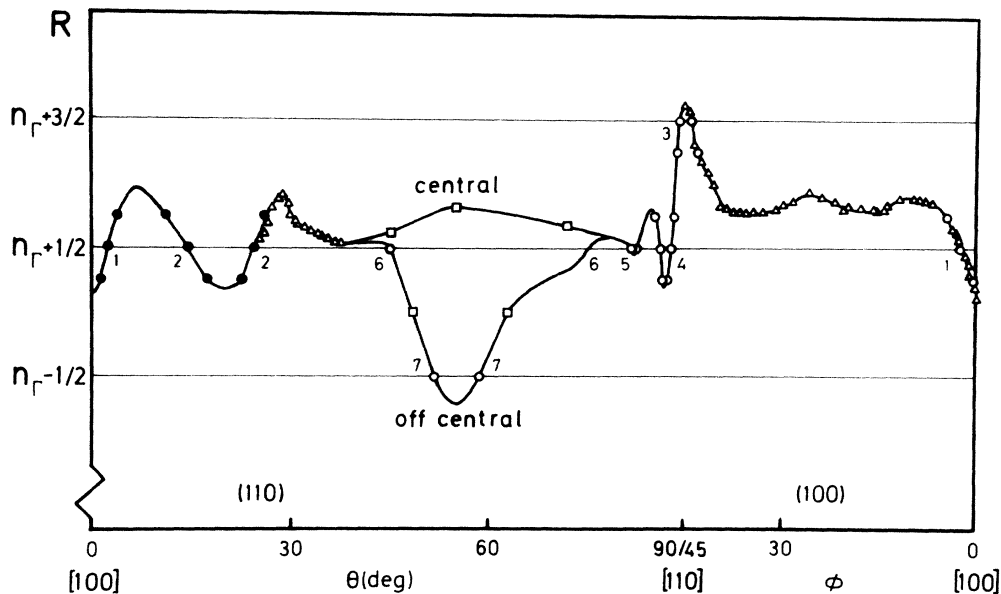


FIG. 2. $R(\theta, \phi)$ in the symmetry planes on the Γ sheet. The curve in the (110) plane out to 26° is taken from Ref. 1. SSZ's from Ref. 1 (●), Ref. 4 and this work (○), data points from amplitude variation (△), and estimated data points as described in the text (□) are indicated in the figure. The occurrence of SSZ's are labeled in accordance with Fig. 1.

the off-center orbit splits off, the central orbit is changing from a maximum to a minimum orbit, meaning that the curvature factor is passing through zero. This should manifest itself as an extreme increase in the amplitude which also was registered. The measured amplitude increases from the SSZ and reaches a maximum at 28° , while the calculated amplitude with the cosine factor equal to 1 has a minimum at 29° . Whether $R(\theta, \phi)$ is actually crossing an integer or is just exhibiting a maximum at 28° cannot be found from the measurements of platinum alone. Studies of the platinum-iron sample, performed under the assumption that the effect of the iron impurities is a monotonic increase of the Zeeman splitting and thus of $R(\theta, \phi)$, did not resolve this ambiguity.

(ii) The second part is the beat-pattern area over [111]. By investigating the beat patterns the amplitude variation of both the central and off-center orbits were measured. Due to the extremely long beat patterns when the off-center orbit splits off, no amplitude measurements were performed in the regions 38° – 41° and 73° – 78° out from [100]. A SSZ contour not earlier reported for the off-center orbit was observed. It cuts through the (110) plane 45° from [100], while between [111] and [110] it disappears into the long-beat region. From observations of the contour out from the mirror plane in this area we extrapolate that the contour cuts the plane at 76° .

In the platinum-iron sample the SSZ contour closest to [111] has moved toward [111] by less than 1.0° . The newly observed contour has also moved toward [111], by 2° between [100] and [111], while it still could not be found between [111] and [110]. From Ref. 8 and this work it is clear that all SSZ contours of the fundamental for the central orbit take the value $R = n_\Gamma + \frac{1}{2}$, except for the small contour around [110] that has a higher integer value, $R = n_\Gamma + \frac{3}{2}$. From this fact and the knowledge of

the slope of R at all the contours and under the assumption that there is no hidden SSZ contour in the noninvestigated beat-pattern area, we conclude that the larger SSZ contour for the off-center orbit also takes $R = n_\Gamma + \frac{1}{2}$ and the smaller $R = n_\Gamma - \frac{1}{2}$.

As in palladium,⁵ the amplitudes for the central orbit for both the pure and the diluted sample have maxima at [111] and thus $R(\theta, \phi)$ has a maximum or minimum close to an integer value at [111]. To reveal whether the bend of $R(\theta, \phi)$ is downward or upward, the amplitude out from [111] was compared to the amplitude at [111] for both platinum and platinum-iron. The relative amplitude in platinum out from [111] was found to be lower than that in platinum-iron, indicating that the upward bend is the most probable case. This conclusion is also reached when comparing ratios between the amplitudes of the central and the off-center orbits. Between the SSZ contours of the off-center orbit, the amplitude reaches a maximum when $R(\theta, \phi)$ takes an integer value. The ratios between the central and off-center orbits at these positions are much higher in platinum-iron than in platinum, indicating that $R(\theta, \phi)$ for the central orbit has increased to a value closer to an integer.

Studies of other parts of the Γ sheet indicate that the shift in $R(\theta, \phi)$ for the platinum-iron sample is in the range 0.10–0.15, and since the amplitude for this sample shows that $R(\theta, \phi)$ does not exceed an integer value at [111], the fractional part of $R(\theta, \phi)$ for pure platinum at [111] is estimated to 0.80–0.85 (central orbit). The calculated amplitude is fairly constant from [111] out to 75° from [100], while it increases by 30% when going from [111] to 45° from [100], nearly independent of the value of the Dingle temperature. The measured amplitude variation for the central orbit then gives that $R(\theta, \phi)$ is $n_\Gamma + 0.6$ at 45° and $n_\Gamma + 0.7$ at 75° (see Fig. 2). To com-

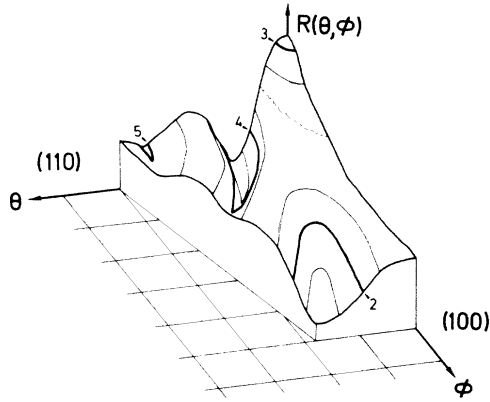


FIG. 3. Anisotropy of $R(\theta, \phi)$ for the Γ sheet demonstrated in the area around $[110]$. The spacing between the contours is 0.25. SSZ contours for the fundamental (thick solid line, labeled according to Fig. 1), second harmonic (thin solid line), and amplitude maximum where R is an integer (dashed line) are shown. All contours have been observed experimentally except the contour for the second harmonic furthest out in the (110) plane. Since the absolute value of R is unknown, the (θ, ϕ) plane does not constitute a zero value. The grid in this plane is 3×3 deg.

bine this with the results in the previous part one must conclude that a maximum in $R(\theta, \phi)$ at 28° is the most likely interpretation.

(iii) The third part is the area around $[110]$. In the earlier work⁴ the change of the integer of $R(\theta, \phi)$ between the SSZ contours was unknown. The study of the platinum-iron sample performed in this work shows that the closed SSZ contour around $[110]$ is extended, on the average, by 0.3° , meaning $R(\theta, \phi) = n_\Gamma + \frac{3}{2}$, while the width of the contour at 87° in the (110) plane has shrunk from 1.7° to 1.4° and the small contour at 82° has been substituted by a minimum, thus indicating that both these contours have the value $n_\Gamma + \frac{1}{2}$. However, the minimum is not located between the locations for the two SSZ's in pure platinum, but has shifted approximately half a degree toward $[110]$ to 83.0° . This was observed twice with the sample reorientated in between and may originate from an anisotropy in the increase of the Zeeman splitting. The SSZ's of the fundamental together with the SSZ's of the second harmonic give a clear picture of the variation of $R(\theta, \phi)$ in this region, as can be seen in Fig. 3.

The α orbit

The variation of R for the α orbit is established from earlier measurements,^{1,4,7,8} and in this work a few complementary studies have been performed. An additional SSZ of the fundamental compared with those reported earlier was observed 36.5° from $[100]$ in the (100) plane. The angle for the SSZ contour of the second harmonic closest to $[100]$ was determined to be 20.6° . Further studies of the second harmonic have not been performed, although several more SSZ's could be expected.

To determine if n_α is even or odd at $[100]$, and thus eliminate half of the possible n_α values, a measurement of

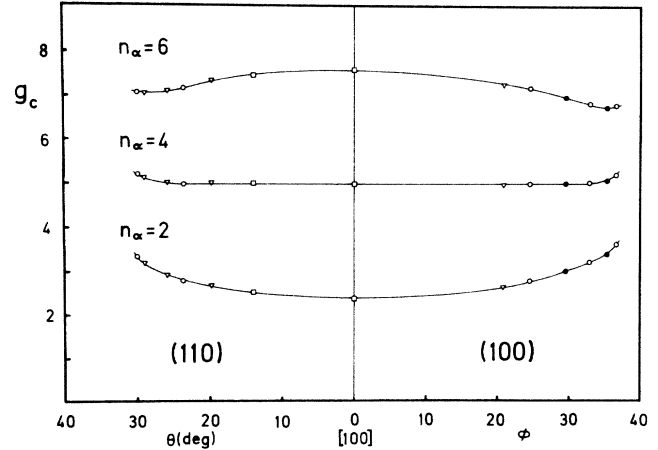


FIG. 4. g_c for the α orbit in the symmetry planes for different choices of n_α . As shown, $n_\alpha = 4$ gives a very isotropic g_c . SSZ's on the fundamental (\circ), second harmonic (∇), data points from amplitude variation (\square), and maximum amplitudes (\bullet) are indicated in the figure. The points in the (110) plane are taken from Ref. 1. Effective masses from Ketterson and Windmiller (Ref. 7) have been used to extract g_c from R

the phase at infinite field (ψ_∞) was performed. This was done at 14 different fields between 2.5 and 6.7 T by calculating a mean value of 10 observations of the phase at each field. An extrapolation to infinite field resulted in $\psi_\infty = 0.84 \pm 0.04$, which is consistent with an even value of n_α . The most isotropic g_c is found for $n_\alpha = 4$ as demonstrated in Fig. 4.

DISCUSSION

General

When interpreting the spin-splitting argument it is straightforward to associate the fundamentally existing difference in extremal areas ΔA between spin-up and spin-down sets of Landau levels with the parameter R . When solving E_z or g_c from the relation $R = E_z/E_L = g_c m_c/2$, one must be aware of the electron-phonon-interaction effect. R is, in the same way as the magnetization, not affected by this effect. The electron-phonon effect will, however, change m_c and thus E_L , which is found in experiment. It will also effect E_z (at E_F), when it is defined as the energy difference between two Landau levels with the same number of oscillations remaining to infinite magnetic field. If the effective mass m_c is enhanced, E_z (or g_c) will decrease correspondingly, thus leaving R unchanged. This can be found from simple geometrical arguments (Fig. 5). As an alternative one may ignore the electron-phonon effects and use the calculated effective mass, which cannot be measured. E_z will then constitute the energy difference between spin-up and spin-down bands without electron-phonon interaction. We have chosen the first alternative to avoid including calculated corrections (band-structure masses) in the data presented.

The lack of theoretical calculations of the g factor becomes clear when interpreting the results. However, a

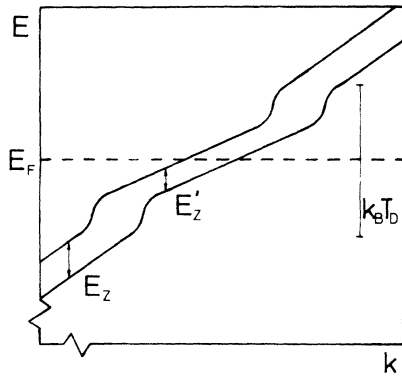


FIG. 5. Schematic figure showing the effect of electron-phonon interaction valid for $k_B T_D \gg E_Z$, T_D being the Debye temperature. The magnetic field splits the spin-up and spin-down energy bands by E_Z . The disturbance from the electron-phonon interaction is tied to the Fermi level (E_F), and the local energy splitting at E_F is E'_Z . The two Zeeman splittings, averaged for a cyclotron orbit, are related through $E_Z = (m_c/m_c^b)E'_Z$, where m_c^b is the cyclotron band mass. The electron-paramagnon interaction can be treated similarly.

qualitative treatment of the data is in some cases an appropriate approach, for instance when comparing g_c and its variation as such over the Γ sheet and α orbit. The clear anisotropy on the Γ sheet (Fig. 6) is in marked contrast with the almost isotropic behavior of the α orbit. A difference in the g_c factors may in this case be correlated to the wave-function character of the sheets. The Γ sheet is built up by Bloch states in the energy region where the broad s band crosses the close-lying d bands, making this sheet severely affected by s - d hybridization while the part of the open hole sheet where the α orbit exists has pure d character.⁹

It is interesting to make a comparison with palladium. Platinum and palladium have very similar band structures and their Fermi surfaces consist of nearly identical sheets. Also, in palladium the α orbit has a rather isotropic g_c while the Γ sheet exhibits large anisotropy.⁵ However, in palladium g_c does not vary as fast with angle as it does in platinum. The differences in the band structure of plati-

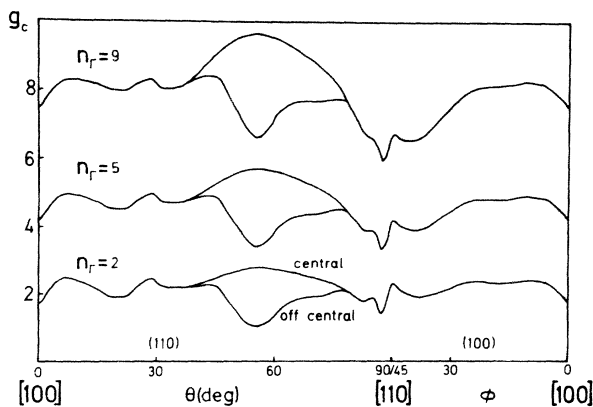


FIG. 6. g_c vs θ extracted from the $R(\theta, \phi)$ curve in Fig. 2. Since n_Γ is unknown, a set of g_c curves with different n_Γ is presented.

num and palladium are mainly the width of the d bands and the spin-orbit-coupling parameter λ_d . A qualitative measure of the g shift is given by $\lambda_d/\Delta E$ (Ref. 10), where ΔE is the energy difference between the Fermi level and the nearest lower-lying energy band. Since ΔE may vary over the Fermi surface the parameter λ_d/W , where W is the width of the d bands, is preferred when comparing average g shifts between different elements.^{11,12} Platinum has 35% broader d bands than palladium and a spin-orbit-coupling parameter that is 4 times larger,⁹ implying that λ_d/W is 3 times larger in platinum than in palladium. This indicates that the band-structure effects may introduce a greater anisotropy of g_c in platinum as compared to palladium. In addition to these effects an anisotropic contribution to g_c from the many-body enhancement can also be expected and, theoretically, it has been demonstrated in palladium.¹³

The absolute value of g_c cannot be measured when using the dHvA effect. However, the magnetic susceptibility can be used to provide an average value of the local spin-splitting factor, and this average value can give a hint as to in what region the integer n lies. It has been estimated that the measured susceptibility for platinum equals the enhanced Pauli susceptibility for the d electrons. All other contributions cancel out.¹⁴ The value of the enhancement given in the literature varies, but 3.6 (Ref. 15) is a reasonable estimate. With the enhancement given as $(g_{\text{eff}}/2)^2 S$, S being the Stoner enhancement and g_{eff} including relativistic effects, an average g factor is found as $\langle g \rangle \equiv g_{\text{eff}} S = 4(3.6)/g_{\text{eff}}$. Using a calculated value for $g_{\text{eff}} = 2.14$ (Ref. 12) and compensating $\langle g \rangle$ for the electron-phonon interaction by the factor $D_{\text{BS}}/D_{\text{SH}} = 0.62$, D_{BS} being the density of states derived from a band-structure calculation and D_{SH} that found from specific-heat measurements,^{7,16} one gets $\langle g \rangle = 4.2$.

The Γ sheet

The strong variation of $R(\theta, \phi)$ is most striking, especially the oscillatory behavior around $[110]$ with a maximum value at $[110]$. This top is, however, to a great extent, a result of the variation of the effective mass, and when extracting g_c for different values of n_Γ it is revealed that the surroundings of $[110]$ have low g_c values for all integers n_Γ with a small local maximum at $[110]$. For this extraction the effective-mass values given in Ref. 7 have been used, except for the off-center orbit, for which the masses have been taken from Ref. 17. When $\langle g \rangle = 4.2$, then $n_\Gamma = 5$ is the most likely integer, but since the contribution to the magnetic susceptibility from the Γ sheet is low, depending on its small part of the total density of states, n_Γ may differ from this value.

When comparing the g_c curves for platinum with the results for palladium,⁵ a profound similarity in the gross feature is found. There is a variation in g_c from $[100]$ to approximately 30° out in both mirror planes which is rather small compared with the maximum over $[111]$ for the central orbit and the deep minimum for the off-center orbit, and the minimum at $[110]$ for the central orbit. This similarity is to a large part hidden in the $R(\theta, \phi)$ curves because of the difference in the anisotropy of the

effective masses.

When interpreting g_c measurements it must be remembered that although the g_c values are average values of the spin splitting for the different Bloch states that are passed by the cyclotron orbit, there is no way to make an inversion from the g_c factors to point g factors if the tensor nature is considered. The g factor associated with each Kramer-degenerated k point possesses a tensor nature, and, in general, different spin splittings are expected for different field directions.^{11,18,19} Despite this we think that it is possible to associate a relatively higher or lower value of the local g factor with specific directions out from our results.

The Γ sheet in platinum is highly affected by s - d hybridization with some exceptions; the [100] and [111]

directions are almost pure d -like.⁹ If these directions are correlated with a lower value of g than the average value, and the [110] direction with a slightly higher, one finds that g_c at [100] should be a small minimum since four each of the [100] and [110] directions are passed [Fig. 7(a)]. Also, the maximum and minimum at [111] and [110], respectively, may then be explained since six of the higher-valued [110] points are passed for the [111] direction [Fig. 7(b)] and six of the low-valued [100] and [111], but only two [110] points for the magnetic field in the [110] direction [Fig. 7(c)]. There are few theoretical works on g factors. Mueller *et al.*¹¹ have calculated some point g factors, including band-structure effects but not many-body effects. For a magnetic field perpendicular to a (100) plane, the [100] direction has $g(\mathbf{k}_F, \hat{\mathbf{B}}) = 0.40$ while

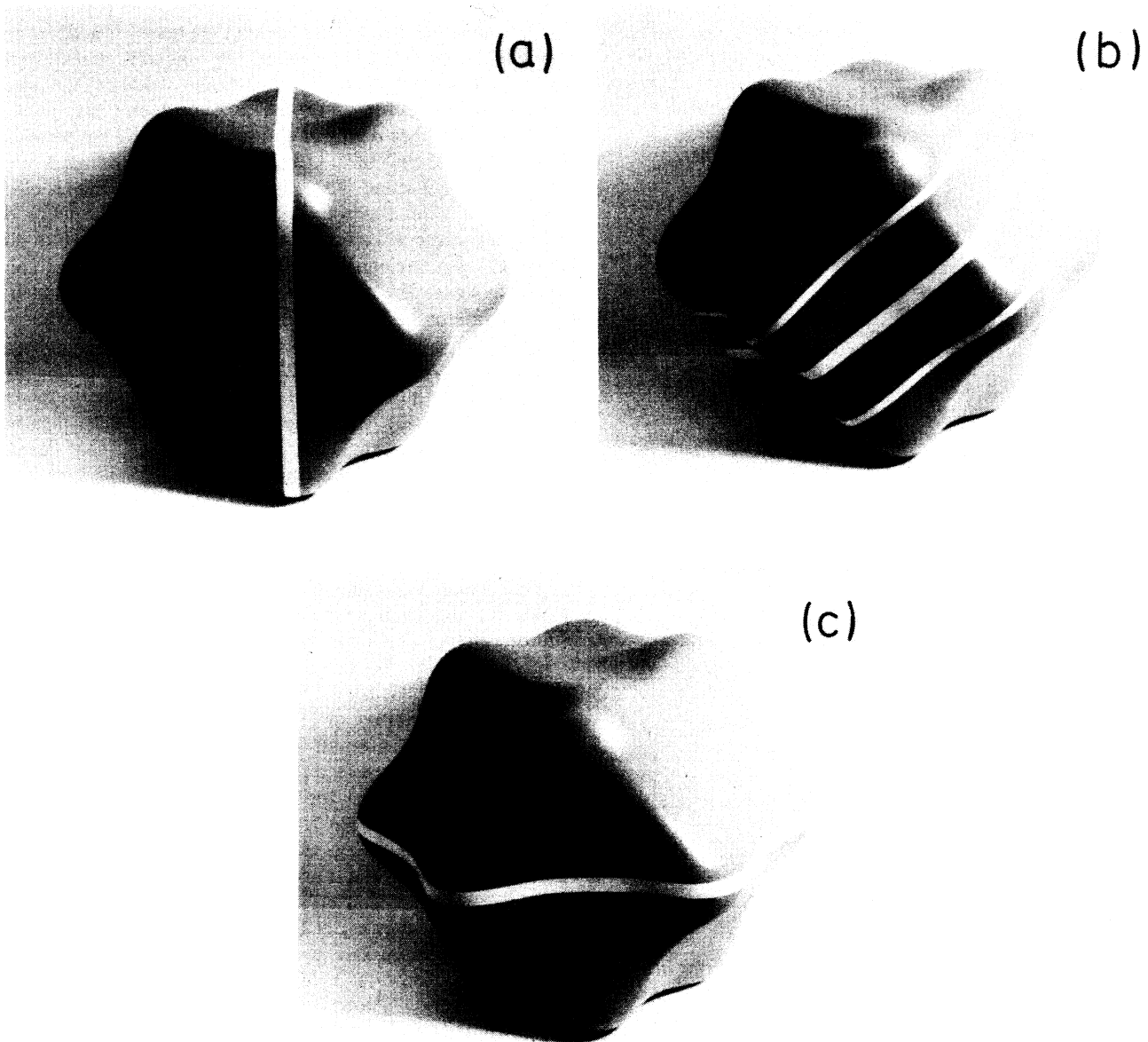


FIG. 7. Cyclotron orbit on the Γ sheet for the magnetic field in a (a) [100] direction and (b) [111] direction. The two off-center orbits (thin lines) are shown together with the central orbit. (c) [110] direction.

a parallel field gives $g(\mathbf{k}_F, \hat{\mathbf{B}}) = 1.38$. For cyclotron orbits the magnetic field is always in a perpendicular direction. Under this condition Mueller *et al.* gives $g(\mathbf{k}_F, \hat{\mathbf{B}})$ at a [110] direction as equal to 1.13, nearly 3 times higher than the value for the [100] direction and in agreement with our qualitative estimate. It should be pointed out that the lowest value of g_c is actually found 3° out from [110], while [110] exhibits a local maximum.

Regarding the minimum for the off-center orbit at [111], one finds that the cyclotron orbit is climbing the [111] bumps on the Fermi surface. For the [111] direction the cyclotron orbit almost passes over the bumps, giving a low g_c value as for the [110] direction [see Figs. 6 and 7(b)].

The α orbit

The SSZ contours follow the effective-mass contours that are lying as circles around [100]. This implies that the cyclotron orbits along the SSZ contours have constant g_c factors. As demonstrated in Fig. 4, the choice $n_\alpha = 4$ gives an almost isotropic g_c with a value close to 4.9. The estimated $\langle g \rangle$ is in agreement with this value.

CONCLUSIONS

These rather extended measurements of the conduction-electron g_c factor in platinum have, together with the earlier measurements on palladium, given a clear picture of the variation of the cyclotron spin splitting over various parts of the Fermi surface. It has been shown earlier that the two elements are very similar in many aspects, ranging from the topology of the Fermi surface^{7,9,20} to magnetic susceptibility features.²¹ It is now also demon-

strated that the variations of g_c are very similar. We find that the strong anisotropy on the Γ sheets is connected with the s - d hybridization to some extent, but that the extreme values are correlated to unhybridized states: s character in palladium and d character in platinum. It is worth noting that the difference between the maximum and the minimum values of g_c in the symmetry planes is approximately 35% for palladium and 40% for platinum (using reasonable values of n_F). Although band-structure effects on the g factor are expected to be larger in platinum than in palladium and vice versa regarding the exchange enhancement, we find profound similarities in the behavior of the Zeeman splitting.

For the α orbit an isotropic g_c factor can be deduced for both platinum and palladium through a proper choice of n_α . Under such an assumption the value of n_α has to be at least twice as large for palladium,⁵ which only partly could be explained by the difference in the effective masses. Therefore, g_c should then be larger for the α orbit in palladium than in platinum.

Even if the spin-orbit interaction is believed to cause the main part of the anisotropy of g_c , an anisotropy of the exchange enhancement is probably not negligible, at least not in palladium. Therefore it is essential to include this effect in theoretical works.

ACKNOWLEDGMENTS

Dr. S. P. Hörnfeldt is gratefully acknowledged for his continuous interest in the work and for valuable discussions. We are very grateful to Dr. L. Ohlsén for giving professional help to make a plaster model of the Γ sheet. The work has been supported by the Swedish National Research Council.

- ¹S. P. Hörnfeldt, L. Nordborg, G. W. Crabtree, and W. R. Johanson, *Phys. Scr.* **25**, 688 (1982).
- ²S. Engelsberg and G. Simpson, *Phys. Rev. B* **2**, 1657 (1970).
- ³I. M. Lifshitz and A. M. Kosevitch, *Zh. Eksp. Teor. Fiz.* **29**, 730 (1955) [*Sov. Phys.—JETP* **2**, 636 (1956)].
- ⁴P. Gustafsson, H. Ohlsén, L. Nordborg, and S. Hörnfeldt, *Solid State Commun.* **45**, 395 (1983).
- ⁵H. Ohlsén, P. Gustafsson, L. Nordborg, and S. Hörnfeldt, *Phys. Rev. B* **29**, 3022 (1984).
- ⁶G. W. Crabtree, L. R. Windmiller, and J. B. Ketterson, *J. Low Temp. Phys.* **20**, 655 (1975).
- ⁷J. B. Ketterson and L. R. Windmiller, *Phys. Rev. B* **2**, 4813 (1970).
- ⁸L. Nordborg, M. Dronjak, K. Gramm, and S. P. Hörnfeldt, *J. Magn. Magn. Mater.* **23**, 323 (1981).
- ⁹O. K. Andersen, *Phys. Rev. B* **2**, 883 (1970).
- ¹⁰R. J. Elliott, *Phys. Rev. B* **96**, 266 (1954).
- ¹¹F. M. Mueller, A. J. Freeman, and D. D. Koelling, *J. Appl.*

Phys. **141**, 1229 (1970).

- ¹²A. H. MacDonald, *J. Phys. F* **12**, 2579 (1982).
- ¹³T. Jarlborg and A. J. Freeman, *Phys. Rev. B* **23**, 3577 (1981).
- ¹⁴A. M. Clogston, V. Jaccarino, and Y. Yafet, *Phys. Rev.* **134**, A650 (1964).
- ¹⁵F. Y. Fradin, D. D. Koelling, A. J. Freeman, and T. J. Watson-Yang, *Phys. Rev. B* **12**, 5570 (1975).
- ¹⁶M. Dixon, F. E. Hoare, T. M. Holden, and D. E. Moody, *Proc. R. Soc. London, Ser. A* **285**, 561 (1965).
- ¹⁷J. B. Ketterson and L. R. Windmiller, *Phys. Rev. Lett.* **20**, 321 (1968).
- ¹⁸M. H. Cohen and E. T. Blount, *Philos. Mag.* **5**, 115 (1960).
- ¹⁹Y. Yafet, in *Solid State Physics*, edited by F. Seitz and D. Turnbull (Academic, New York, 1963), Vol. 14, pp. 1–89.
- ²⁰L. R. Windmiller, J. B. Ketterson, and S. Hörnfeldt, *Phys. Rev. B* **3**, 4213 (1971).
- ²¹S. Foner, R. Dorlo, and E. J. McNiff, Jr., *J. Appl. Phys.* **39**, 551 (1968).

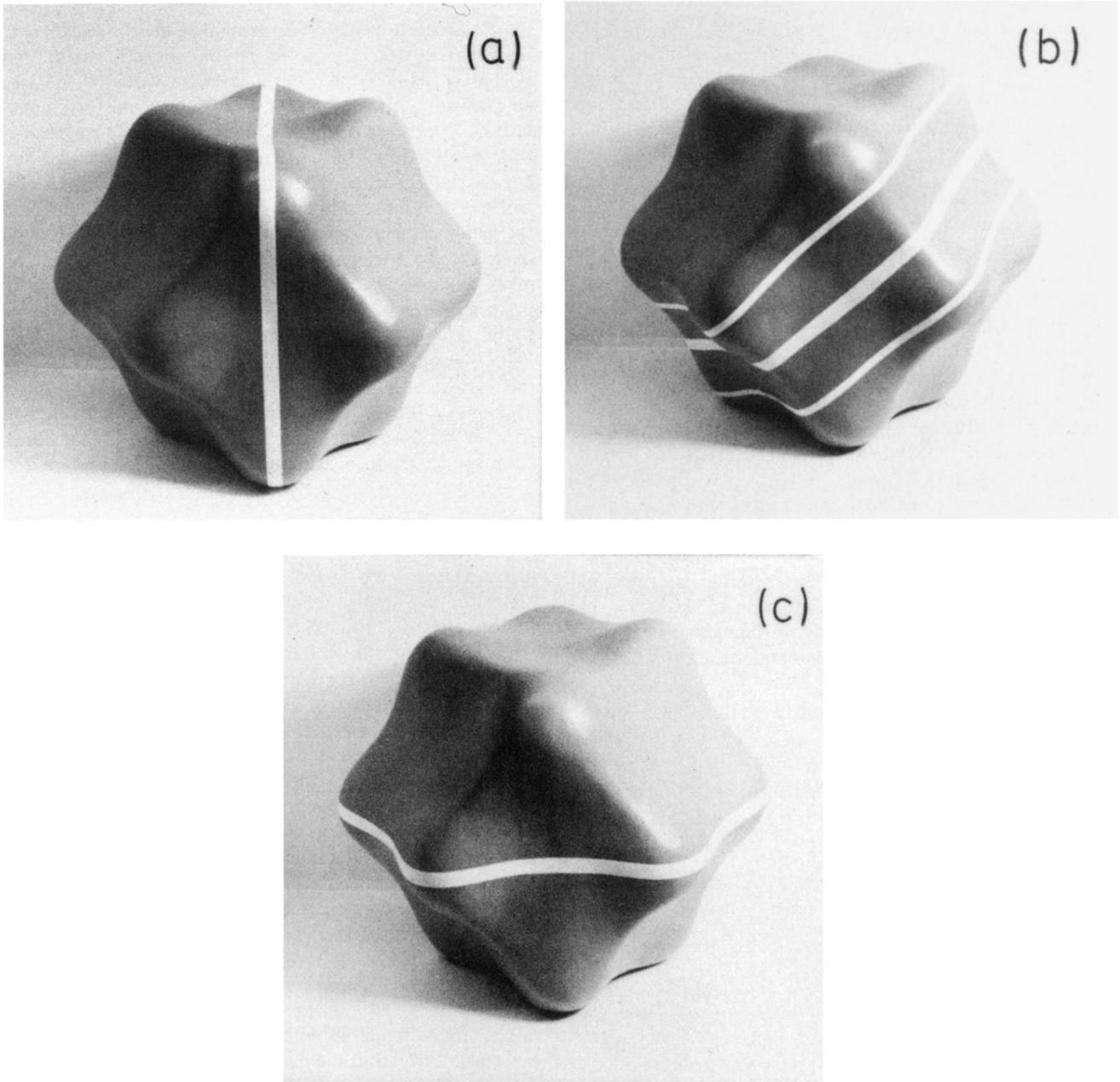


FIG. 7. Cyclotron orbit on the Γ sheet for the magnetic field in a (a) $[100]$ direction and (b) $[111]$ direction. The two off-center orbits (thin lines) are shown together with the central orbit. (c) $[110]$ direction.